

Reductive Quantum Phase Estimation

Nicholas J.C. Papadopoulos,^{1, 2,*} Jarrod T. Reilly,¹ John Drew Wilson,¹ and Murray J. Holland¹

¹*JILA, NIST, and Department of Physics, University of Colorado, 440 UCB, Boulder, CO 80309, USA*

²*Department of Computer Science, University of Colorado, 440 UCB, Boulder, CO 80309, USA*

(Dated: February 8, 2024)

Estimating a quantum phase is a necessary task in a wide range of fields of quantum science. To accomplish this task, two well-known methods have been developed in distinct contexts, namely, Ramsey interferometry (RI) in atomic and molecular physics and quantum phase estimation (QPE) in quantum computing. We demonstrate that these canonical examples are instances of a larger class of phase estimation protocols, which we call reductive quantum phase estimation (RQPE) circuits. Here we present an explicit algorithm that allows one to create an RQPE circuit. This circuit distinguishes an arbitrary set of phases with a fewer number of qubits and unitary applications, thereby solving a general class of quantum hypothesis testing to which RI and QPE belong. We further demonstrate a trade-off between measurement precision and phase distinguishability, which allows one to tune the circuit to be optimal for a specific application.

I. INTRODUCTION

For over a century, physics has benefited greatly from exploiting interference effects between waves [1, 2]. In particular, the accurate estimation of a relative phase between parts of a wavefunction is a pivotal task in numerous fields of quantum physics and quantum computing. For example, the central goal of quantum metrology is to construct experimental platforms capable of making high-precision measurements of the quantum phase that correspond to a physical parameter [3–5]. Progress in this area has led to the development of quantum sensors that have then been used in a wide range of groundbreaking technologies, from atomic clocks [6, 7] to medical devices [8, 9]. In quantum information science, there exist important algorithms that seek to calculate the quantum phase as precisely as possible in a single measurement. This can be used to find the eigenvalues of a unitary operator, thereby allowing one to perform computations such as matrix inversion and modular multiplication with a quantum advantage [10–12]. For example, it is a crucial step in the Harrow-Hassidim-Lloyd linear system of equations algorithm [13, 14] as well as the crux of Shor’s algorithm for prime factorization [10, 15].

Due to the far-reaching impact of estimating a quantum phase, various techniques have been developed to accomplish this task. For example, in quantum metrology the standard method is Ramsey interferometry (RI) [16]. In RI, with a direct correspondence to optical interferometers, a single qubit is split into a coherent superposition, undergoes unitary encoding of a phase, and is then recombined (see Fig. 3(a)). The alternate approach used in quantum computation is founded on Kitaev’s quantum phase estimation (QPE) algorithm [10, 17, 18], which aims to determine the correct phase from a discrete set of possibilities in a single run of a multi-qubit quantum circuit. The QPE algorithm consists of conditional rota-

tions to estimate the quantum phase over small intervals of the Bloch sphere’s equator, and the intervals become exponentially smaller as the number of qubits increases.

Many quantum algorithms have a phase estimation subroutine that ideally estimates an encoded phase θ after a single run of the circuit. This can be accomplished for phases where every qubit in the circuit has unit probability of being in one of the computational basis states (i.e., the bare eigenstates). The canonical QPE algorithm consisting of n qubits can discriminate between a set of 2^n phases evenly distributed throughout the interval $[0, 2\pi]$. However, there are important problems in quantum hypothesis testing [19–23], a central pillar of modern quantum information science research, where one wants to discriminate between a certain discrete set of phases starting with a flat prior probability distribution. In these situations, the QPE circuit is excessive with potentially many unneeded qubits performing unnecessary rotations, increasing the chance of errors to occur during the algorithm through both quantum and classical noise. Furthermore, there are simple situations in which QPE would actually require an infinite number of qubits to distinguish between two phases with certainty after a single run of the circuit, such is the case with $\theta = 0$ and $\theta = \pi/3$.

In this paper, we present an algorithm that generates a phase estimation circuit capable of perfectly discriminating between any set of phases with certainty after a single run, given the phases are rational multiples of π . This allows one to design a phase estimation circuit with fewer qubits and unitary gates than QPE in many cases. This algorithm therefore develops a more general class of phase estimation circuits that we call reductive quantum phase estimation (RQPE), of which RI and QPE are special cases. We demonstrate that RQPE circuits have a trade-off between phase measurement precision for higher distinguishability of phases, which we show is an interpolation between the canonical RI and QPE circuit. This allows one to tune a phase estimation circuit to be optimized for a specific task.

The article is organized as follows. In Sec. II, we in-

* Corresponding author; Nicholas.Papadopoulos@colorado.edu

introduce an algorithm that produces RQPE circuits and demonstrate its use for two illustrative examples. Then in Sec. III, we analyze how to compare different RQPE circuits with a cost-benefit analysis. We show relevant calculations for our analysis of RQPE circuits in Appendix F.

II. RQPE GENERATION ALGORITHM

We begin by presenting an algorithm that generates RQPE circuits. We consider circuits consisting of a set of n qubits, each prepared in the state $|0\rangle$. We label the qubit states $|q_j\rangle$ with index j , and we assume that one can perfectly perform instantaneous, noiseless gates and measurements. The gates used in the RQPE algorithm are the Z gate $Z_j = |0\rangle\langle 0|_j - |1\rangle\langle 1|_j$, powers of the Z gate $Z_j^p = |0\rangle\langle 0|_j + e^{i\pi p}|1\rangle\langle 1|_j$, the Hadamard gate $H_j = (|0\rangle\langle 1|_j + |1\rangle\langle 0|_j + Z_j)/\sqrt{2}$, and powers of the controlled Z-gate with target $|q_j\rangle$ controlled by $|q_k\rangle$: $CZ_{j,k}^p = \mathbb{I}_j \otimes |0\rangle\langle 0|_k + Z_j^p \otimes |1\rangle\langle 1|_k$.

The objective of quantum phase estimation is to accurately estimate an unknown quantum phase θ using minimal resources. In this work, we assume the phase is encoded by Z rotations, such that $U_j = e^{-i\theta Z_j/2}$. Note that we consider circuits that apply the phase shift directly onto the control qubits through U_j , but our results extend to methods that apply the phase shift using any controlled unitary acting on an ancillary register, as is typically done in QPE [10].

We now present an algorithm that generates a circuit that, given some set of phases, Θ with $|\Theta| = T$, which is some subset of $\{\pi f_i = \frac{\pi x_i}{d} : 0 \leq x_i < 2d, x_i \in \mathbb{Z}\}$ where \mathbb{Z} is the set of integers, allows one to determine the encoded phase $\theta \in \Theta$ with certainty after a single run. Here, all f_i are rational and can therefore be rewritten with a common integer denominator d and a set of numerators $S_0 = \{x_i\}$. Starting with $i = 0$, the circuit generating algorithm consists of the sequence enumerated in Algorithm 1.

- (S1) Set G_i as the greatest common divisor (GCD) of the numerators S_i .
- (S2) Set Q_i as $\{y = \frac{x}{G_i} : x \in S_i\}$.
- (S3) Set A_i as the mode of the differences $y_e - y_o$ for all even $y_e \in Q_i \cap 2\mathbb{Z}$ and odd $y_o \in Q_i \cap (2\mathbb{Z} + 1)$ integers. If there are no even integers, $Q_i \cap 2\mathbb{Z} = \emptyset$, A_i is the minimum of Q_i .
- (S4) Set S_{i+1} equal to Q_i with A_i added to the resulting odd integers: $S_{i+1} = \{y_e : \forall y_e \in Q_i \cap 2\mathbb{Z}\} \cup \{y_o + A_i : \forall y_o \in Q_i \cap (2\mathbb{Z} + 1)\}$.
- (S5) Iterate (S1)-(S4) by incrementing i until $S_{i+1} = \{0\}$.

Algorithm 1. Steps of the circuit generating algorithm. Note that the set theory notation ignores repeated elements.

To construct the circuit that distinguishes phases in Θ

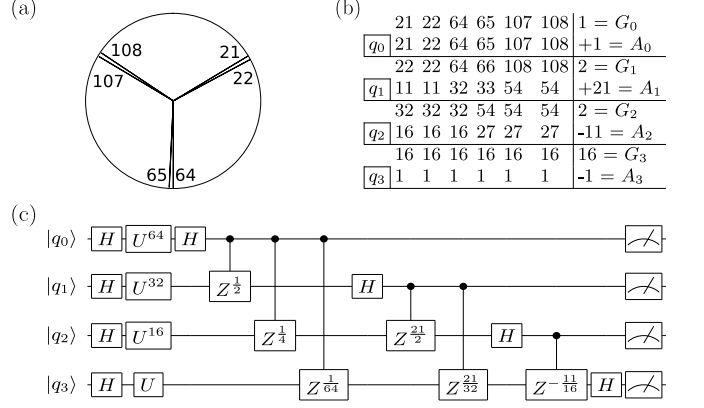


FIG. 1. (a) Visualization of $\Theta = \{\frac{\pi x}{64} : x \in \{21, 22, 64, 65, 107, 108\}\}$ around the equator of the Bloch sphere. (b) Application of Algorithm 1 to find G_i and A_i for all iterations. (c) The circuit generated by Algorithm 1 by way of Eq. (1).

with certainty after a single run, the gate sequence (see Appendix A)

$$H_j \left(\prod_{k=0}^{j-1} CZ_{j,k}^{\frac{A_k}{\prod_{\ell=k+1}^j G_\ell}} \right) U_j^{\frac{d}{\prod_{\ell=0}^j G_\ell}} H_j |q_j\rangle, \quad (1)$$

is applied on each $|q_j\rangle$. Here, the application of the H and CZ gates across all qubits after the unitary applications is reminiscent of the QFT^\dagger gate (see Appendix H), QFT standing for the quantum Fourier transform, which can be found in Ref. [10]. Performing a measurement on $|q_j\rangle$ produces a measurement outcome $m_j \in \{0, 1\}$, and the measurement of all n qubits produces a binary string $m_0 \dots m_{n-1}$. This binary string gives an estimation of θ (see Appendix B):

$$\theta_{\text{est}} = -\frac{\pi}{d} \sum_{j=0}^{n-1} m_j A_j \prod_{k=0}^j G_k. \quad (2)$$

We note that RQPE circuits can be run sequentially on a single qubit that is reset to $|0\rangle$ after performing each line of the circuit, and each measurement effectively modifies the encoded phase in subsequent unitary applications. The sequential approach is explored in more depth in Refs. [24, 25] and is effectively equivalent to the multi-qubit, parallel circuits presented here. In Appendix C we analyze the time and space complexity of the generated circuits from Eq. (1) as well as Algorithm 1. Here, we find that the circuit generating algorithm runs in polynomial time with respect to T and $\log_2 h$, where $h = \max[S_0]$, and the number of qubits needed is upper bounded by $O(\min[T, \log_2 h])$.

A common situation in which the RQPE circuits of Eq. (1) can be very useful for hypothesis testing is systems where an external perturbation splits degenerate energy levels. As an example, we consider a system in which $|1\rangle$ is physically a $F = 1$ hyperfine state while

$|0\rangle$ is $F' = 0$. Therefore, a magnetic field will cause a Zeeman energy shift of the $|F = 1, m_F = \pm 1\rangle$ states by $\pm \hbar \delta_B$. Each qubit thus undergoes an additional rotation $\exp[i m_F \delta_B Z_i t/2]$ for a run time t , such that $\theta = \theta' + m_F \delta_B t$. We therefore may wish to distinguish between three locations on the Bloch sphere's equator to determine which transition is being driven, as shown in Fig. 1(a). We thus use Algorithm 1 to create a circuit that can distinguish the set $\Theta = \{\frac{\pi x_i}{64} : x_i \in \{21, 22, 64, 65, 107, 108\}\}$ with certainty after a single run. In Fig. 1(b), we show the outcome of the iterations of Algorithm 1 for this particular set of phases.

In the first iteration, $i = 0$, Algorithm 1 Steps (S1) and (S2) ensures some odd numerators, enabling $|q_0\rangle$ to distinguish between all $\theta_{0,e}$ from all $\theta_{0,o}$ within the set $\{\frac{\pi G_0 x}{64} : 0 \leq x < \frac{128}{G_0}, x \in \mathbb{Z}\}$. Here, j in $\theta_{i,j}$ indicates whether x is even or odd so that all $\theta_{i,e}$ measure 0 with certainty while all $\theta_{i,o}$ measure 1 with certainty on $|q_i\rangle$.

This is accomplished by the unitary rotation U_0^{d/G_0} as it becomes $\exp[-ix_i \pi Z_j / (2G_0)]$ with $x_i/G_0 \in \mathbb{Z}$. The goal of Step (S3) is to pick an addition A_0 such that it reduces the size of the set of integers as much as possible, i.e., it converts the maximum amount of odd integers to even integers in the set. This addition dictates the controlled rotation on subsequent qubits. Step (S4) then returns a new set of integers S_1 from which one finds a new GCD, G_1 , in the next iteration. This allows one to distinguish between all $\theta_{1,e}$ from all $\theta_{1,o}$ within the set $\{\frac{\pi G_1 G_0 x}{64} : 0 \leq x < \frac{128}{G_1 G_0}, x \in \mathbb{Z}\}$. Step (S5) iterates this process such that each iteration corresponds to a qubit in the generated circuit.

Using this reduction process in conjunction with Eq. (1), we produce the circuit displayed in Fig. 1(c) to distinguish the phases in Θ , where the final symbol stands for an individual qubit measurement in the Z -basis. Note that only four qubits are used to distinguish the desired phases in RQPE with certainty after a single run. This can be compared to seven qubits needed in QPE, since $2d = 2^7$, demonstrating the utility of our circuit generation algorithm. Furthermore, while running it once can determine which $\theta \in \Theta$ is encoded, running it many times and using some statistical analysis such as Bayes theorem [16, 26] reliably estimates any continuous θ within the desired ranges.

Another interesting feature of Algorithm 1 can be demonstrated with the example shown in Fig. 2. Here, we use the circuit generation algorithm to distinguish the phases $\Theta \in \{\frac{\pi x_i}{70} : x_i \in \{66, 93, 108, 123, 138\}\}$ with certainty after a single run. As shown in Fig. 2(b), we find a set of only odd numerators in the line for $|q_2\rangle$. This ensures that, for all phases in Θ , the qubit $|q_2\rangle$ will always be in the $|1\rangle$ state when the measurement is performed. Therefore, this qubit can be removed from the circuit while $CZ_{j,2}^p$ gates can be replaced with uncontrolled Z_j^p gates. When estimating the original theta, consider this qubit as if it had existed and measured 1, i.e. $m_2 = 1$. We label $|q_2\rangle$ as a “phantom” qubit and display the reduced circuit where we have removed the phantom qubit

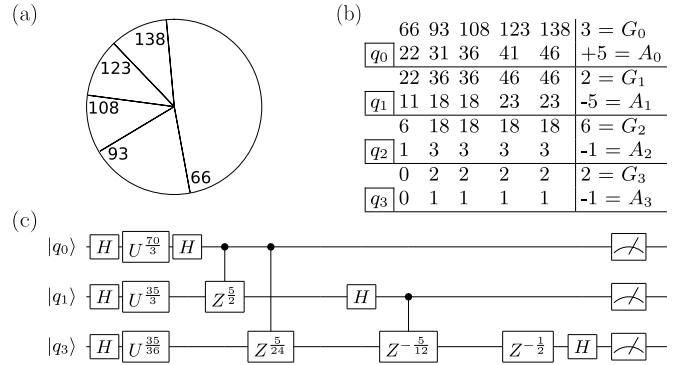


FIG. 2. (a) Visualization of $\Theta = \{\frac{\pi x}{70} : x \in \{66, 93, 108, 123, 138\}\}$ around the equator of the Bloch sphere. (b) Application of Algorithm 1 to find G_i and A_i for all iterations. (c) The circuit generated by Algorithm 1 by way of Eq. (1) and removing phantom qubits.

$|q_2\rangle$ in Fig. 2(c). One can see that the last qubit in Fig. 1 is a phantom qubit as well.

Removing a phantom qubit from a circuit does not decrease distinguishability of the discrete phases in Θ and does not necessarily decrease distinguishability of continuous phase estimation. We see, for example, that it does not affect distinguishability within the desired ranges in Fig. 1. Precision, on the other hand, will be affected due to Eq. (4).

III. TRADE-OFF BETWEEN PRECISION AND DISTINGUISHABILITY

RQPE circuits can be compared by three key properties: the number of unitary applications, distinguishability, and precision. Interestingly, the extremes of this circuit generation algorithm create circuits for both RI and QPE, and these serve as perfect examples to showcase these comparable properties. RI will be automatically generated from Algorithm 1 when $|\Theta| = 2$, the smallest possible size, while QPE will be automatically generated when $|\Theta| = 2d$, the largest possible size. We display the circuit diagrams for these procedures in Figs. 3(a) and 3(c).

In order to compare circuits in general, we use the total number of unitary applications, r , during a single run as the constrained resource. This can be written as a sum over all qubits, $r = \sum_{j=0}^{n-1} u_j$, where u_j represents the number of applications of U_j to $|q_j\rangle$. In this way, QPE has $r_{\text{QPE}} = 2^n - 1$, and RI has $r_{\text{RI}} = u_0$. One way to compare an RI circuit to QPE would then be to set $r_{\text{RI}} = r_{\text{QPE}}$, thereby applying $(U_0)^{r_{\text{QPE}}}$ on the qubit in RI, and compare the resulting precision and distinguishability. We consider an optimal circuit to be one that minimizes the number of unitary applications while achieving some desired precision and distinguishability, as discussed in more detail in Appendix F.

Let M_k be the measured binary string corresponding

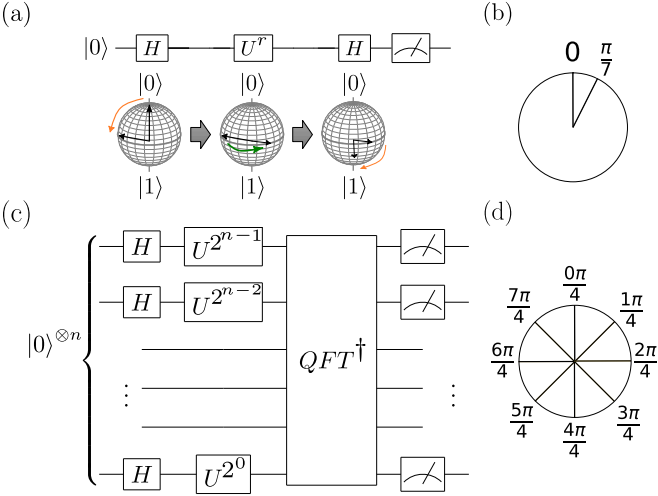


FIG. 3. Canonical phase estimation procedures. (a) RI circuit with the corresponding Bloch sphere rotations. (b) The perfectly distinguishable phases of RI with 7 unitary applications. (c) QPE circuit. (d) The perfectly distinguishable phases of QPE with 3 qubits.

to the n -qubit measurement outcome in the measurement basis $\mathcal{M} = \{M_k : k \in \mathbb{Z}, 0 \leq k < 2^n\}$. If, for each $\theta_i \in \Theta$, there exists a unique measurement outcome M_k with conditional probability $P(M_k|\theta_i) = 1$, and for all $\theta_j \in \Theta$ with $\theta_j \neq \theta_i$ the same measurement outcome M_k has conditional probability $P(M_k|\theta_j) = 0$, then we say the circuit perfectly distinguishes the set of phases Θ , i.e., distinguishes them with certainty after a single run of the circuit.

In general, every phase estimation circuit has a unique set of phases which it can perfectly distinguish. In RI, one can perfectly distinguish exactly $T = 2$ phases, $\Theta = \{0, \frac{\pi}{r_{\text{RI}}}\}$, as these are the points where the Ramsey fringes reach their extremum values (see Fig. 4(a)). For the example circuits we consider, this corresponds to $\theta \in \{0, \frac{\pi}{2}\}$ on the equator of the Bloch sphere as shown in Fig. 3(b). Conversely, the QPE algorithm can perfectly distinguish the phases $\Theta = \{\frac{\pi x}{2^{n-1}} : x \in \mathbb{Z}, 0 \leq x < 2^n\}$, such that $T = 2^n$. This feature of QPE can be seen in Fig. 4(b), where one has $T = 8$ perfectly distinguishable phases corresponding to the eight possible measurement outcomes for $n = 3$ qubits. These perfectly distinguishable phases are shown on the equator of the Bloch sphere in Fig. 3(d).

Using quantum state geometry (adapted from Eq. (1.57) in [27]), one can define the distance between two phases, θ_a and θ_b , using the l_2 -distance between conditional probabilities in a measurement basis \mathcal{M} :

$$\mathcal{D}_{\mathcal{M}}(\theta_a, \theta_b) = \sqrt{\frac{1}{2} \sum_{k=0}^{2^n-1} [P(M_k|\theta_a) - P(M_k|\theta_b)]^2}. \quad (3)$$

When $\mathcal{D}_{\mathcal{M}}(\theta_a, \theta_b) = 1$, this is the maximum distance corresponding to two perfectly distinguishable phases,

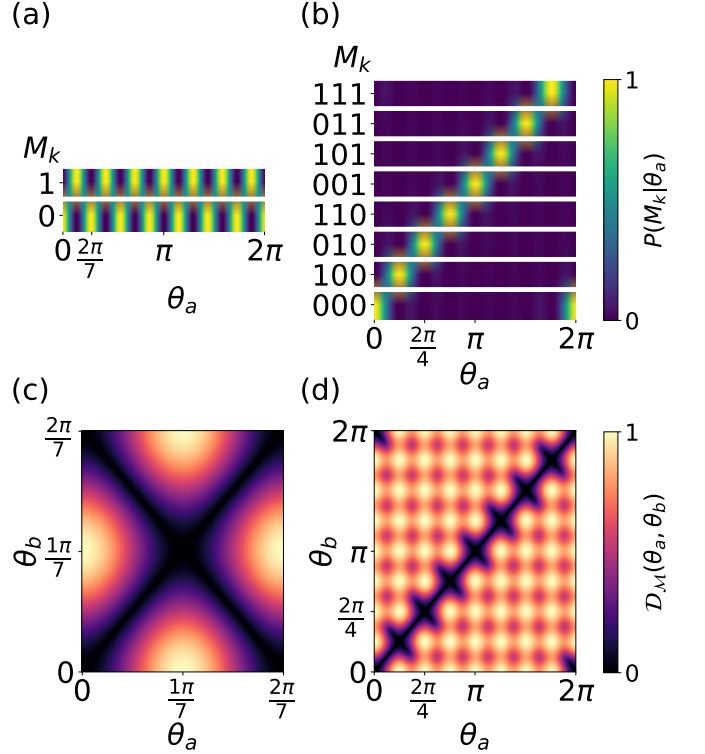


FIG. 4. The conditional probability of (a) RI with 7 unitary applications and (b) QPE with 3 qubits. The distance between phases θ_a and θ_b calculated by Eq. (3) for (c) RI with 7 unitary applications and (d) QPE with 3 qubits.

whereas $\mathcal{D}_{\mathcal{M}}(\theta_a, \theta_b) = 0$ corresponds to two phases which cannot be distinguished. In Figs. 4(c) and 4(d), we compare RI and QPE using the distance metric in Eq. (3) and measurements in the Z -basis.

While QPE has a larger range of distinguishable phases than RI, this is not the only figure of merit that one wishes to optimize when performing phase estimation. In the context of quantum metrology, one performs many runs of the circuit to measure θ from a continuous set of phases, $\Theta_c = \{x \in \mathbb{R}, 0 \leq x < 2\pi\}$, with greater and greater accuracy. Therefore, another important metric of phase estimation circuits is the precision. This is nicely encapsulated by the classical Fisher information (CFI) [28] with a given measurement basis $\mathcal{I}(\theta|\mathcal{M})$, as the maximal achievable precision over R runs of the circuit is given by the Cramér-Rao bound [29], $\Delta\theta^2 \propto 1/\sqrt{R\mathcal{I}_{\mathcal{M}}}$. For the circuits we consider, the CFI for the Z -basis is given by (see Appendix E)

$$\mathcal{I}(\theta|\mathcal{M}) = \sum_{j=0}^{n-1} u_j^2. \quad (4)$$

One can see that the CFI is dominated by the qubit that has the largest number of unitary applications. This $\max[u_j]$ in QPE is only on the order of half of $\max[u_j]$ in RI when $r_{\text{RI}} = r_{\text{QPE}}$ because RI has all of its unitary applications acting on a single qubit. Therefore, QPE

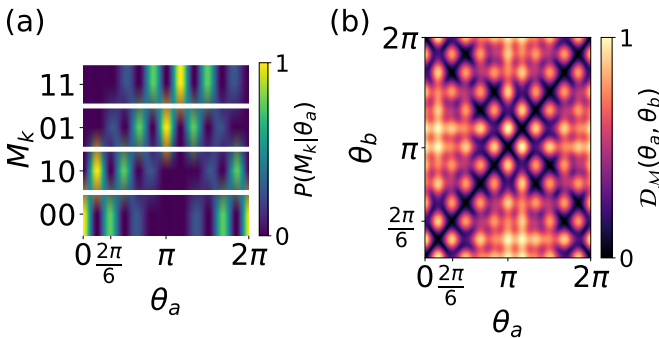


FIG. 5. Using an RQPE circuit with 1 and 6 unitary applications on two qubits, shown are (a) the conditional probability and (b) the distance calculated by Eq. (3) between two phases.

will have on the order of half as much precision given the same number of unitary applications. This can be seen in Figs. 4(a) and 4(b) by the width of the fringes.

In a general RQPE circuit with n qubits, one can perfectly distinguish $T \leq 2^n$ phases. However, the phases need not be evenly distributed around the equator of the Bloch sphere, as is the case with QPE, since the exponential on the unitary gate applications over subsequent qubits are not restricted to powers of two. Therefore, there is a trade-off between distinguishability and precision that can be tuned for a given parameter estimation objective by employing different RQPE circuits. As with the canonical examples, RQPE circuits can either be run once for perfect distinguishability between the phases in Θ or can be run multiple times to estimate a continuous phase.

We consider an example circuit in Fig. 5, which is a two-qubit circuit with $|q_0\rangle$ and $|q_1\rangle$. We use the unitaries U_0^6 and U_1 to match the number of unitary applications used in the canonical circuits studied in Fig. 3. The probability distribution for different phases is displayed in Fig. 5(a). Since the CFI is dominated by $\max[u_j]$, we expect this RQPE circuit, having $\max[u_j] = 6$, to have a higher precision than QPE with $\max[u_j] = 4$, but lower than RI with $\max[u_j] = 7$. This is confirmed in Fig. 5(a) where we compare the width of the first fringe to that of the canonical circuits.

Meanwhile, the opposite relationship is true when comparing the circuit's distinguishability. We show this in Fig. 5(b) where we calculate Eq. (3) for our RQPE circuit. We say that a circuit is more distinguishable if it has a greater number of θ_i having a distance of 0 to only itself rather than additionally having a distance of 0 to some other θ_j . Then, this RQPE circuit can be com-

pared to Figs. 4(a) and 4(b) for the canonical examples to see that it is more distinguishable than RI but less distinguishable than QPE.

There are two notable features of distinguishability in RQPE circuits, further analyzed in Appendix G. One is the repetition of probability distributions. This is determined by the qubit with the lowest number of unitary applications causing the probability distributions over the range $[0, \frac{2\pi}{\min[u_j]}]$ to repeat over the full 2π range, being truncated after 2π . The second distinguishability feature is the distinguishability within this repeated range, which is determined by the distribution of unitary applications over the qubits. The generation algorithm that we have presented in this paper utilizes these two features with the goal of optimizing the distribution of unitary applications for any given Θ .

IV. CONCLUSION AND OUTLOOK

In this article, we have demonstrated that a general class of quantum phase estimation algorithms, which we labeled as RQPE, exist that encompass the canonical examples of RI and QPE. Furthermore, by casting these canonical examples into the language of RQPE we are able to compare these distinct algorithms on equal footing. The figures of merit that we considered were precision, determined by the CFI in Eq. (4), and the distinguishability, determined by the distance in Eq. (3). The figures of cost that we considered were the number of unitary applications and the number of qubits. We found that RI is more sensitive than QPE when constrained to the same number of unitary applications, but QPE is more distinguishable than RI. We demonstrated that these are two extremes of RQPE circuits, and so one can find a middle ground between these examples by tuning a trade-off between these two figures of merit.

While the presented circuit generation algorithm can be used to improve current phase estimation standards, it is not necessarily optimal in all cases. Future work may therefore be directed towards either reducing complexity in the generation algorithm or increasing optimality in the generated circuits.

ACKNOWLEDGMENTS

The authors thank John Cooper and Bo Waggoner for useful discussions. This research was supported by NSF OMA 1936303; NSF PHY 1734006; NSF OMA 2016244; NSF 2231377; and .

[1] A. A. Michelson and E. W. Morley, American Journal of Science **s3-34**, 333–345 (1887).

[2] E. Jahrgang, *Zeitschrift für Instrumentenkunde*, Vol. 1881 (Springer, 1891).

[3] L. Pezzè, A. Smerzi, M. K. Oberthaler, R. Schmied, and P. Treutlein, *Rev. Mod. Phys.* **90**, 035005 (2018).

[4] C. L. Degen, F. Reinhard, and P. Cappellaro, *Rev. Mod. Phys.* **89**, 035002 (2017).

[5] J. T. Reilly, J. D. Wilson, S. B. Jäger, C. Wilson, and M. J. Holland, *Phys. Rev. Lett.* **131**, 150802 (2023).

[6] C. W. Chou, D. B. Hume, T. Rosenband, and D. J. Wineland, *Science* **329**, 1630 (2010).

[7] T. Bothwell, C. J. Kennedy, A. Aeppli, D. Kedar, J. M. Robinson, E. Oelker, A. Staron, and J. Ye, *Nature* **602**, 420 (2022).

[8] N. Aslam, H. Zhou, E. K. Urbach, M. J. Turner, R. L. Walsworth, M. D. Lukin, and H. Park, *Nature Reviews Physics* **5**, 157–169 (2023).

[9] M. A. Taylor and W. P. Bowen, *Physics Reports* **615**, 1 (2016), quantum metrology and its application in biology.

[10] M. A. Nielsen and I. L. Chuang, Phase estimation, in *Quantum Computation and Quantum Information* (Cambridge University Press, 2010) p. 221–226.

[11] M. T. Quintino, Q. Dong, A. Shimbo, A. Soeda, and M. Murao, *Phys. Rev. Lett.* **123**, 210502 (2019).

[12] S.-M. Cho, A. Kim, D. Choi, B.-S. Choi, and S.-H. Seo, *IEEE Access* **8**, 213244 (2020).

[13] A. W. Harrow, A. Hassidim, and S. Lloyd, *Phys. Rev. Lett.* **103**, 150502 (2009).

[14] X.-D. Cai, C. Weedbrook, Z.-E. Su, M.-C. Chen, M. Gu, M.-J. Zhu, L. Li, N.-L. Liu, C.-Y. Lu, and J.-W. Pan, *Phys. Rev. Lett.* **110**, 230501 (2013).

[15] P. Shor, in *Proceedings 35th Annual Symposium on Foundations of Computer Science* (1994) pp. 124–134.

[16] N. F. Ramsey, *Phys. Rev.* **78**, 695 (1950).

[17] A. Y. Kitaev, *Electron. Colloquium Comput. Complex.* **TR96** (1995).

[18] L. Pezzè and A. Smerzi, *PRX Quantum* **2**, 040301 (2021).

[19] K. M. Audenaert, J. Calsamiglia, R. Munoz-Tapia, E. Bagan, L. Masanes, A. Acin, and F. Verstraete, *Physical review letters* **98**, 160501 (2007).

[20] K. M. Audenaert, M. Nussbaum, A. Szkoła, and F. Verstraete, *Communications in Mathematical Physics* **279**, 251 (2008).

[21] J. Calsamiglia, R. Munoz-Tapia, L. Masanes, A. Acin, and E. Bagan, *Physical Review A* **77**, 032311 (2008).

[22] G. Spedalieri and S. L. Braunstein, *Physical Review A* **90**, 052307 (2014).

[23] Z. M. Rossi and I. L. Chuang, *Phys. Rev. A* **104**, 012425 (2021).

[24] M. Mosca and A. Ekert, in *Quantum Computing and Quantum Communications*, edited by C. P. Williams (Springer Berlin Heidelberg, Berlin, Heidelberg, 1999) pp. 174–188.

[25] M. Dobšíček, G. Johansson, V. Shumeiko, and G. Wordin, *Phys. Rev. A* **76**, 030306 (2007).

[26] N. Wiebe and C. Granade, *Phys. Rev. Lett.* **117**, 010503 (2016).

[27] I. Bengtsson and K. Życzkowski, Probability and statistics, in *Geometry of Quantum States: An Introduction to Quantum Entanglement* (Cambridge University Press, 2020) p. 25–28.

[28] E. L. Lehmann and G. Casella, *Theory of point estimation* (Springer, 1998) p. 115.

[29] C. R. Rao, Information and the accuracy attainable in the estimation of statistical parameters, in *Breakthroughs in Statistics: Foundations and Basic Theory*, edited by S. Kotz and N. L. Johnson (Springer New York, New York, NY, 1992) pp. 235–247.

[30] E. Bach and J. O. Shallit, The euclidean algorithm: Worst-cases analysis, in *Algorithmic Number Theory*, Vol. 1 (MIT Press, 1997) p. 68–70.

[31] G. H. Hardy and E. M. Wright, *An introduction to the theory of numbers* (Clarendon Press, 1960).

[32] M. G. A. Paris, Quantum estimation for quantum technology (2009), arXiv:0804.2981 [quant-ph].

Appendix A: Gates on a Qubit

Define θ as $\frac{\pi x_a}{d}$. The goal is to perform some operations to change θ so that the j -th qubit measures $e^{-i\pi x_a \mathcal{Z}}$, where x_j is the numerator from the set $\mathcal{A}_j = \{\frac{x}{G_j} : x \in S_j\}$ to which x_a transforms. For x_0 , the algorithm only needs to divide by G_0 , resulting in the following gate

$$\begin{aligned} e^{-i\pi x_0 \mathcal{Z}} &= e^{-i\pi \frac{x_a}{G_0} \mathcal{Z}} \\ &= e^{-i\pi \frac{x_a d}{G_0 d} \mathcal{Z}} \\ &= (e^{-i\pi \frac{x_a}{d} \mathcal{Z}})^{\frac{d}{G_0}} \\ &= U_i^{\frac{d}{G_0}}. \end{aligned} \quad (\text{A1})$$

Now, doing the same process for x_1 , the previous reduction applies as well as A_0 and G_1 , adding A_0 only if the numerator at \mathcal{A}_0 is odd, which happens when $q_0 = 1$.

$$\begin{aligned} x_1 &= \left(\frac{x_a}{G_0} + q_0 A_0\right) \frac{1}{G_1} \\ &= \frac{x_a}{G_0 G_1} + \frac{q_0 A_0}{G_1} \\ &= \frac{x_a d}{G_0 G_1 d} + \frac{q_0 A_0}{G_1} \\ &= \frac{x_a}{d} \frac{d}{G_0 G_1} + \frac{q_0 A_0}{G_1} \end{aligned} \quad (\text{A2})$$

$$\begin{aligned} e^{-i\pi x_1 \mathcal{Z}} &= e^{-i\pi \left(\frac{x_a}{d} \frac{d}{G_0 G_1} + \frac{q_0 A_0}{G_1}\right) \mathcal{Z}} \\ &= \left(e^{-i\pi \frac{x_a}{d} \mathcal{Z}}\right)^{\frac{d}{G_0 G_1}} e^{-i\pi \frac{q_0 A_0}{G_1} \mathcal{Z}} \\ &= U_j^{\frac{d}{G_0 G_1}} Z_j^{\frac{q_0 A_0}{G_1}} \\ &= Z_j^{\frac{q_0 A_0}{G_1}} U_j^{\frac{d}{G_0 G_1}}. \end{aligned} \quad (\text{A3})$$

One can see that this pattern results in the gates for qubit q_j as

$$\begin{aligned} \text{gates}(q_j) &= H_j (Z_j^{\frac{q_0 A_0}{G_1 \dots G_i}} Z_j^{\frac{q_1 A_1}{G_2 \dots G_j}} \dots Z_j^{\frac{q_{j-1} A_{j-1}}{G_j}}) U_j^{\frac{d}{G_0 \dots G_j}} H_j \\ &= H_j \left(\prod_{k=0}^{j-1} CZ_{j,k}^{\frac{A_k}{\prod_{\ell=k+1}^j G_\ell}} \right) U_j^{\frac{d}{\prod_{\ell=0}^j G_\ell}} H_j. \end{aligned} \quad (\text{A4})$$

Appendix B: Estimating θ

Backtracking through the reductions, i.e. subtracting the additions and multiplying by the GCDs, reveals the value assigned to each qubit measurement, which we call the bit value. In a four-qubit circuit, the original numerator will be

$$\begin{aligned}\theta &= \pi((((-m_3 A_3)G_3 - m_2 A_2)G_2 \\ &\quad - m_1 A_1)G_1 - m_0 A_0)G_0 \\ &= \pi(-m_3 A_3 G_3 G_2 G_1 G_0 - m_2 A_2 G_2 G_1 G_0 \\ &\quad - m_1 A_1 G_1 G_0 - m_0 A_0 G_0).\end{aligned}\quad (\text{B1})$$

One can see the pattern that the bit value of each measured bit b_i , which is included in the final estimate if and only if $m_j = 1$, will be

$$b_j = -\frac{\pi}{d} A_j \prod_{k=0}^j G_k. \quad (\text{B2})$$

This allows for the transformation of the measurement results m_0, \dots, m_{n-1} into the unknown theta as

$$\theta = -\frac{\pi}{d} \sum_{j=0}^{n-1} m_j A_j \prod_{k=0}^j G_k \quad (\text{B3})$$

Appendix C: Complexity

Define h as the greatest numerator in S_0 and note that $T \leq 2d$ and $h < 2d$. Each qubit will ideally reduce the size of Θ by half, imposing a lower bound of $\lceil \log_2(T) \rceil$ on the number of qubits, n . Additionally, the algorithm will always be able to reduce at least one theta into another after each measurement, and the final measurement distinguishes two thetas, therefore $n \leq T - 1$.

Moreover, any set of theta numerators is a subset of $\{i : i \in \mathbb{Z} \text{ and } 0 \leq i < 2^{\lceil \log_2 h \rceil + 1}\}$, which can be distinguished using $A = [-1, -1, -1, \dots]$ and $G = [1, 2, 2, 2, \dots]$ with $\lceil \log_2 h \rceil + 1$ qubits. If one restricts the additions used in the classical generation algorithm negative, then the number of qubits will always be less than or equal to this. However, allowing positive additions further optimizes many circuits, and since we cannot guarantee this constraint in this case, it can be trivially ensured by using these A and G values if the generated circuit uses more qubits than this. This puts a second upper bound on n , resulting in the following bounds.

$$\lceil \log_2(T) \rceil \leq n \leq \min(T - 1, \lceil \log_2 h \rceil + 1) \quad (\text{C1})$$

In the worst case, the generation algorithm will produce this G , resulting in the geometric sequence

$$a_i = d \left(\frac{1}{2}\right)^i \quad (\text{C2})$$

where a_i is the number of unitary applications on q_i . This series results in an upper bound on the total number of unitary applications, r , in one run of the circuit as

$$r < 2d \quad (\text{C3})$$

Each reduction in the generation algorithm is composed of first finding the GCD of the set of thetas. Finding the GCD of two numbers a and b can be done using the Euclidean GCD Algorithm in $O(\log_2 \min(a, b))$ time [30]. The algorithm can then perform this iteratively for all the possible thetas in a set, achieving a time complexity of $O(T \log_2 h)$.

The second phase of a reduction consists of finding a value to add to the odd numerators which reduces the set size as much as possible. The method described in this paper runs in at most $O(T^2)$ time, since in the worst case there will be an equal number of even and odd thetas, $\frac{T}{2}$, and each odd will be added to each even, producing $\frac{T^2}{4}$ results. Each result is then counted to find the mode, which results in a total of $\frac{T^2}{4}$ time in the worst case.

Each multiplication and addition can be considered to run in constant time (assuming all numbers fit into the word size of the hardware) over each theta, so the operations after finding a GCD or addition can be done in time $O(2T)$.

The combination of all of these steps within an iteration multiplied by the number of iterations necessary results in a total time complexity of $O((T^2 + T \log_2 h) \cdot \min(T, \log_2 h))$ to generate the quantum circuit. Let's look at each case more specifically. In the case that $T \leq \log_2 h$:

$$\begin{aligned}O((T^2 + T \log_2 h) \cdot T) &= O(T^3 + T^2 \log_2 h) \\ &= O(T^2(T + \log_2 h)) \\ &= O(T^2 \log_2 h)\end{aligned}\quad (\text{C4})$$

because $\log_2 h$ is the larger term in $(T + \log_2 h)$. In the case that $T \geq \log_2 h$:

$$\begin{aligned}O((T^2 + T \log_2 h) \cdot \log_2 h) &= O(T^2 \log_2 h + T(\log_2 h)^2) \\ &= O(T \log_2 h(T + \log_2 h)) \\ &= O(T^2 \log_2 h)\end{aligned}\quad (\text{C5})$$

because T is the larger term in $(T + \log_2 h)$. Therefore, both cases end up being the same and produce a runtime of

$$O(T^2 \log_2 h). \quad (\text{C6})$$

The algorithm stores the possible thetas and two arrays for the GCDs and additions in each reduction, which are all on the order $O(T)$. In this paper's method to find a particular addition in a reduction step, however, the algorithm stores $O(T^2)$ possibilities to consider, which is the dominant factor. This equates to a total space complexity of $O(T^2)$.

Appendix D: Building a Circuit from Bit Values

The goal of the circuit-building reductions is to find the A s and G s. If one is given the bit values instead of a Θ set, thereby distinguishing Θ consisting of all possible subset sums of these bit values, one can find these values with much more simplicity. First, find S_0 and d , which can be done by first finding the fraction forms using the continued fractions algorithm [31].

Then, set $G_0 = \text{GCD}(S_0)$ and $A_0 = \frac{S_{0,0}}{G_0}$, where $S_{0,j}$ is the j th numerator corresponding to b_j . Next, set $G_1 = \text{GCD}(\{\frac{S_{0,j}}{G_0} : j \geq 1\})$ and $A_1 = \frac{S_{0,1}}{G_0 G_1}$. Continue this way until all G s and A s are found.

Note that all A must be odd valued and all G , except G_0 , must be even valued for the presented circuit generation to be sure to work correctly. If these do not hold, then the presented circuit generation algorithm likely cannot be used to distinguish a Θ set matching these bit values exactly.

For example, if one wanted to build a circuit that distinguishes thetas in the range $[0, \frac{2\pi}{d}]$ in even multiples of $\frac{\pi}{d}$, one could use the bit values $b = [\frac{3}{d}, \frac{6}{d}, \frac{12}{d}]$.

$$G_0 = \text{GCD}(S_0) = 3 \quad (\text{D1})$$

$$A_0 = \frac{S_{0,0}}{G_0} = \frac{3}{3} = 1 \quad (\text{D2})$$

$$G_1 = \text{GCD}\left(\left\{\frac{S_{0,1}}{G_0}, \frac{S_{0,2}}{G_0}\right\}\right) = \text{GCD}\left(\left\{\frac{6}{3}, \frac{12}{3}\right\}\right) = \text{GCD}(\{2, 4\}) = 2 \quad (\text{D3})$$

$$A_1 = \frac{S_{0,1}}{G_0 G_1} = \frac{6}{3 \cdot 2} = 1 \quad (\text{D4})$$

$$G_2 = \text{GCD}\left(\left\{\frac{S_{0,2}}{G_0 G_1}\right\}\right) = \text{GCD}\left(\left\{\frac{12}{3 \cdot 2}\right\}\right) = 2 \quad (\text{D5})$$

$$\begin{aligned} A_2 &= \frac{S_{0,2}}{G_0 G_1 G_2} \\ &= \frac{12}{3 \cdot 2 \cdot 2} \\ &= 1 \end{aligned} \quad (\text{D6})$$

Since only the first G is odd and all the A are odd, this b is valid, and these A s and G s may be used in the rest of the circuit generation.

Appendix E: Fisher Information

As explored in [25], RQPE circuits may be equivalently run sequentially on a single qubit, so each line in the circuit will be run separately from each other. This means that each line of the circuit can be considered a Ramsey Interferometry (RI) circuit with additional Z-rotation gates. These rotation gates have the following effect

$$\begin{aligned} H(Z^{z_0} Z^{z_1} \dots) U^r H |0\rangle &= H(Z^{z_0+z_1+\dots}) U^r H |0\rangle \\ &= H Z^j U^r H |0\rangle \\ &= \frac{1}{2} \left[1 + e^{-i(r\theta+j)} \right] \end{aligned} \quad (\text{E1})$$

where z_i is the power of the i th Z-rotation gate, and j is a simplifying variable $j = \sum_{i=0} z_i$.

Let $R[a]$ be the a -th element of Eq. (E1), and let a^* mean the conjugate of a . The classical Fisher information of Eq. (E1) is then (see [32])

$$\begin{aligned} \mathcal{I}_{\mathcal{M}}(\text{RI}) &= \sum_{a=0}^1 \frac{\left(\frac{\partial}{\partial\theta}(R[a]R[a]^*)\right)^2}{R[a]R[a]^*} \\ &= \frac{\left(\frac{\partial}{\partial\theta}(\cos\left(\frac{r\theta+j}{2}\right))^2\right)^2}{(\cos\left(\frac{r\theta+j}{2}\right))^2} + \frac{\left(\frac{\partial}{\partial\theta}(\sin\left(\frac{r\theta+j}{2}\right))^2\right)^2}{(\sin\left(\frac{r\theta+j}{2}\right))^2} \\ &= \frac{\left(-\frac{r}{2}\sin(r\theta+j)\right)^2}{(\cos\left(\frac{r\theta+j}{2}\right))^2} + \frac{\left(\frac{r}{2}\sin(r\theta+j)\right)^2}{(\sin\left(\frac{r\theta+j}{2}\right))^2} \\ &= \frac{r^2}{4} \left(\frac{(\sin(r\theta+j))^2}{(\cos\left(\frac{r\theta+j}{2}\right))^2} + \frac{(\sin(r\theta+j))^2}{(\sin\left(\frac{r\theta+j}{2}\right))^2} \right) \\ &= r^2 \left(\left(\sin\left(\frac{r\theta+j}{2}\right)\right)^2 + \left(\cos\left(\frac{r\theta+j}{2}\right)\right)^2 \right) \\ &= r^2 \end{aligned} \quad (\text{E2})$$

where r is the number of unitary applications on the qubit. One can see that the Fisher information of an RI circuit is irrespective of the embedded θ or j . Hence, additional rotation gates on a Ramsey line have no effect on the Fisher information of that line, and we may simply add the Fisher information of all lines in the RQPE

circuit to calculate the full Fisher information with

$$\mathcal{I}_M(RQPE) = \sum_{i=0}^{n-1} u_i^2. \quad (E3)$$

Appendix F: Examples of Comparing Optimality

We define a phase estimation problem as desiring some precision, defined by the Cramer-Rao bound, while being able to distinguish some range of thetas, $0 \leq \theta \leq h$ in $e^{-i\theta\mathcal{Z}}$ where h is the largest phase, after many runs. This is because if there were separate ranges, RI would still need to distinguish one large range that covers all the separate ranges. A more optimal circuit achieves both of these things while using fewer unitary application and qubits. Define precision as $\frac{1}{p}$ where $p \geq 1$ and $h = \frac{a}{d}$. The precision is defined by the Cramer-Rao bound, so $\frac{1}{p} = \frac{1}{\sqrt{t}\mathcal{I}}$, where t is the total number number of runs and \mathcal{I} is the classical Fisher information.

First, we see what Ramsey Interferometry (RI) requires. RI optimally satisfies these requirements with $r = \frac{1}{h} = \frac{d}{a}$ unitary applications per run. Increasing this shrinks the dynamic range to be less than the required theta range, and distinguishability is lost, while decreasing this exponentially increases the total number of runs to achieve the same precision, resulting in more unitary applications overall. Since the classical Fisher information is $(\frac{d}{a})^2$ according to Eq. (4), we have

$$\begin{aligned} \frac{1}{p} &= \frac{a}{d\sqrt{t}} \\ t &= \left\lceil \left(\frac{pa}{d} \right)^2 \right\rceil, \end{aligned} \quad (F1)$$

taking the ceiling because t is an integer, meaning RI requires $\left\lceil \left(\frac{pa}{d} \right)^2 \right\rceil$ runs to satisfy the requirements. Since each RI run uses exactly one qubit, it requires the same number of qubits. The total number of unitary applications it needs across all runs is therefore

$$\frac{d}{a}t \geq \frac{p^2a}{d}. \quad (F2)$$

Quantum phase estimation (QPE) always has full distinguishability and achieves at least the desired precision when it's most precise qubit reaches it, which happens after 1 run when

$$\begin{aligned} \frac{1}{p} &= \frac{1}{\sqrt{\mathcal{I}}} \\ p &\geq u_{max} \end{aligned} \quad (F3)$$

where u_{max} is the number of unitary applications on the most precise qubit. Since the unitary applications for each qubit in QPE follow powers of two, the most precise qubit having $2^{\lceil \log_2 p \rceil} \leq 2^{\log_2(p)+1}$ unitary applications satisfies the precision requirement. This, in turn, results

in less than $4p$ total unitary applications across all qubits and $\lceil \log_2 p \rceil + 1$ total qubits.

We now have circuits for both RI and QPE that satisfy the distinguishability requirement, so, in order for QPE to outperform RI, we find a precision where the total number of unitary applications for QPE is less than that of RI.

$$\begin{aligned} 4p &< \frac{p^2a}{d} \\ 4p &< p^2h \\ \frac{4}{p} &< h \end{aligned} \quad (F4)$$

This means that QPE is guaranteed to use fewer unitary applications whenever the highest theta is at least four times the desired precision, i.e. when you would like to estimate theta using at least 4 bins of equal spacing.

We do a similar analysis for RQPE. If one wanted to split the range into between some positive integer k and $k+1$ bins, we have

$$\begin{aligned} \frac{1}{p} &= \frac{b}{c}h \\ &= \frac{ba}{cd} \end{aligned} \quad (F5)$$

where $\frac{c}{k+1} < b < \frac{c}{k}$. One could, for example, run the CDA with $\Theta = \left\{ \frac{bax_i}{cd} : x_i \in \mathbb{Z}, 0 \leq x_i \leq k+1 \right\}$, which satisfies the precision and distinguishability requirements after a single run. We will compare the optimality of this circuit, which uses

$$\begin{aligned} r_{RMQPE} &= \frac{cd}{ba} \left(1 + \frac{1}{2} + \frac{1}{4} + \cdots + \frac{1}{2^{\lceil \log_2 k \rceil}} \right) \\ &= \frac{cd}{ba} \left(2 - \frac{1}{2^{\lceil \log_2 k \rceil}} \right) \end{aligned} \quad (F6)$$

Since RI requires

$$\begin{aligned} t &= \left\lceil \left(\frac{pa}{d} \right)^2 \right\rceil \\ &= \left\lceil \left(\frac{cda}{bad} \right)^2 \right\rceil \\ &= \left\lceil \left(\frac{c}{b} \right)^2 \right\rceil \\ &> k^2 \\ &\geq k^2 + 1 \end{aligned} \quad (F7)$$

runs to reach the desired precision, RI is more optimal

than this RQPE circuit when

$$\begin{aligned} \left\lceil \left(\frac{c}{b} \right)^2 \right\rceil \left(\frac{d}{a} \right) &< \frac{cd}{ab} \left(2 - \frac{1}{2^{\lfloor \log_2 k \rfloor}} \right) \\ \left\lceil \left(\frac{c}{b} \right)^2 \right\rceil &< \frac{c}{b} \left(2 - \frac{1}{2^{\lfloor \log_2 k \rfloor}} \right) \\ k^2 + 1 &< \frac{c}{b} \left(2 - \frac{1}{2^{\lfloor \log_2 k \rfloor}} \right) \\ b &< \frac{c}{k^2 + 1} \left(2 - \frac{1}{2^{\lfloor \log_2 k \rfloor}} \right) \end{aligned} \quad (\text{F8})$$

When $k = 0$, the given RQPE circuit simply returns RI, so they are equally optimal. For $k = 1$, we see that RI is more optimal when $b < \frac{3c}{4}$, i.e. one wants a precision of $\frac{3}{4}h$. For $k = 2$, $b < \frac{3c}{10}$, which violates $b > \frac{c}{3}$. This violation persists for all $k > 1$. Therefore, this RQPE circuit is always more optimal than RI except for in the very specific case when one wants $\frac{3}{4}h < \frac{1}{p} \leq h$.

Appendix G: Features of Indistinguishability

For all reductive quantum phase estimation circuits, a single qubit can distinguish between a phase of 0 and $\frac{\pi}{u_i}$ with certainty. However, it also creates a range $\left[0, \frac{2\pi}{\max[1, \min[u_j]]}\right)$ where each θ within it results in an identical Bloch sphere positions as $\theta + j \frac{2\pi}{\max[1, \min[u_j]]} : j \in \mathbb{N}, j < \max[1, u_i]$, where \mathbb{N} are the natural numbers. That is, on the full 2π range of possible thetas, there will be $\max[1, u_i]$ sets of physically indistinguishable thetas after the unitary applications. We call this range the repeated range, \mathcal{S} , and we call this principle of indistinguishable sets “indistinguishability due to repetition”. This can be extended to a multi-qubit RQPE circuit, where

$$\mathcal{S} = \frac{2\pi}{\max[1, \min[u_j]]} \quad (\text{G1})$$

as $\min[u_j]$ has the largest repeated range, and no repetition occurs until repetition over this largest repeated range occurs.

Another type of indistinguishability, which this paper refers to as “indistinguishability due to measurement basis”, is due to identical measurement probability distributions for thetas within the repeated range itself. This means that thetas may lie on different points in the Bloch sphere after the unitary applications but have identical probability distributions given the measurement basis. This is the type of distinguishability that can be increased by distributing unitary applications across multiple qubits in certain ways. This is also the type that is

plotted in our distance graphs, since this distinguishability is simply repeated as the repeated range repeats.

Appendix H: RQPE as a Gate

In the same way that the H and CZ gates after the unitary applications of a QPE circuit can be viewed as a QFT^\dagger gate, one can view the H and CZ gates after the unitary applications of an RQPE circuit as a $(RQPE_{G,A})^\dagger$ gate. In the following definitions, we include SWAP gates to reverse the order of qubits as the final step in the $(RQPE_{G,A})^\dagger$ gate, while keeping the definition of b_i unchanged, in order to more closely match the traditional definition of the QFT gate. However, to match the circuit given in the paper, i.e. without final SWAP gates, \tilde{b} (defined below) should be exchanged with b in the following equations.

The $RQPE_{G,A}$ gate, given some GCDs G and additions A , maps a quantum state $|x\rangle = \sum_{k=0}^{2^n-1} x_k |k\rangle$ to a state $\sum_{k=0}^{2^n-1} y_k |k\rangle$ according to the formula:

$$y_k = \frac{1}{\sqrt{2^n}} \sum_{j=0}^{2^n-1} x_j \exp[i(b \cdot j)(\tilde{u} \cdot k)]. \quad (\text{H1})$$

where the \cdot operation of two operands r and s is $r \cdot s = \sum_{i=0}^{n-1} r_i s_i$, $\tilde{r}_i = r_{n-1-i}$, s_i is the i -th bit of the binary representation of s , b_i is the i -th bit value of the RQPE procedure, and u_i is the number of unitary applications on the i -th qubit, given by

$$u_i = \frac{d}{\prod_{k=0}^i G_k}. \quad (\text{H2})$$

When $|x\rangle$ is a basis state, the $RQPE_{G,A}$ gate can be expressed as the map

$$RQPE_{G,A} : |x\rangle \rightarrow \frac{1}{\sqrt{2^n}} \sum_{k=0}^{2^n-1} \exp[i(b \cdot x)(\tilde{u} \cdot k)] |k\rangle. \quad (\text{H3})$$

The unitary matrix of the $RQPE_{G,A}$ gate acting on quantum state vectors is then

$$\frac{1}{\sqrt{2^n}} \begin{bmatrix} 1 & 1 & 1 & 1 & \dots & 1 \\ 1 & e^{ib_0\tilde{u}_0} & e^{ib_1u_0} & e^{i(b_0+b_1)\tilde{u}_0} & \dots & e^{ic\tilde{u}_0} \\ 1 & e^{ib_0\tilde{u}_1} & e^{ib_1\tilde{u}_1} & e^{i(b_0+b_1)\tilde{u}_1} & \dots & e^{ic\tilde{u}_1} \\ 1 & e^{ib_0(\tilde{u}_0+\tilde{u}_1)} & e^{ib_1(\tilde{u}_0+\tilde{u}_1)} & e^{i(b_0+b_1)(\tilde{u}_0+\tilde{u}_1)} & \dots & e^{ic(\tilde{u}_0+\tilde{u}_1)} \\ \vdots & \vdots & \vdots & \vdots & \ddots & \vdots \\ 1 & e^{ib_0r} & e^{ib_1r} & e^{i(b_0+b_1)r} & \dots & e^{icr} \end{bmatrix}, \quad (\text{H4})$$

where $c = \sum_{i=0}^{2^n-1} b_i$.